

OPEN ACCESS

New Insights Related to Rechargeable Lithium Batteries: Li Metal Anodes, Ni Rich $\text{LiNi}_x\text{Co}_y\text{Mn}_z\text{O}_2$ Cathodes and Beyond Them

To cite this article: Elena Markevich *et al* 2019 *J. Electrochem. Soc.* **166** A5265

View the [article online](#) for updates and enhancements.

You may also like

- [NaH₂PO₄ as an Electrolyte Additive for Enhanced Thermal Stability of LiNi_{0.8}Co_{0.1}Mn_{0.1}O₂/Graphite Batteries](#)
Minsang Jo, Seong-Hyo Park and Hochun Lee
- [Understanding anion-redox reactions in cathode materials of lithium-ion batteries through *in situ* characterization techniques: a review](#)
Ye Yeong Hwang, Ji Hyun Han, Sol Hui Park *et al.*
- [Investigation of Moisture Content, Structural and Electrochemical Properties of Nickel-Rich NCM Based Cathodes Processed at Ambient Atmosphere](#)
Julian K. Mayer, Fabienne Huttner, Carina A. Heck *et al.*

Investigate your battery materials under defined force!
The new PAT-Cell-Force, especially suitable for solid-state electrolytes!



- Battery test cell for force adjustment and measurement, 0 to 1500 Newton (0-5.9 MPa at 18mm electrode diameter)
- Additional monitoring of gas pressure and temperature

www.el-cell.com +49 (0) 40 79012 737 sales@el-cell.com

EL-CELL[®]
electrochemical test equipment





New Insights Related to Rechargeable Lithium Batteries: Li Metal Anodes, Ni Rich $\text{LiNi}_x\text{Co}_y\text{Mn}_z\text{O}_2$ Cathodes and Beyond Them

Elena Markevich,¹ Gregory Salitra,¹ Pascal Hartmann,² Joern Kulisch,² Doron Aurbach,^{1,*} Kang-Joon Park,³ Chong S. Yoon,⁴ and Yang-Kook Sun^{3,**}

¹Department of Chemistry, Bar-Ilan University, Ramat-Gan, 290002 Israel

²BASF SE, Ludwigshafen 67056, Germany

³Department of Energy Engineering, Hanyang University, Seoul 04763, Korea

⁴Department of Materials Science and Engineering, Hanyang University, Seoul 04763, Korea

The electro-mobility revolution challenges the batteries community to develop rechargeable batteries with the highest energy density, including the use of Li metal anodes. Relevant cathode materials include sulfur and molecules with the general formula $\text{LiNi}_x\text{Co}_y\text{Mn}_z\text{O}_2$, denoted as Ni rich NCM ($x+y+z = 1$; $x > 0.5$). We discuss herein new insights obtained from our recent work with cells comprising Li metal anodes, $\text{LiNi}_{0.6}\text{Co}_{0.2}\text{Mn}_{0.2}\text{O}_2$ and LiNiO_2 cathodes with practical charge density higher than 3 mAh/cm². Highly stable behavior of Li metal anodes was realized in solutions containing mono-fluorinated ethylene carbonate (FEC) as a co-solvent. We found that the same solutions stabilize Ni rich NCM cathodes as well. We discuss herein the limiting factor of Li-LiNiO₂ cells in terms of cycle life and have gained new understandings related to failure and stabilization mechanisms of Ni rich NCM cathodes. Providing that the electro-mobility revolution succeeds, we may encounter a shortage in the availability of nickel. We suggest herein strategies for handling this problem by the use of Mn based cathodes.

© The Author(s) 2019. Published by ECS. This is an open access article distributed under the terms of the Creative Commons Attribution 4.0 License (CC BY, <http://creativecommons.org/licenses/by/4.0/>), which permits unrestricted reuse of the work in any medium, provided the original work is properly cited. [DOI: 10.1149/2.0261903jes]



Manuscript submitted October 29, 2018; revised manuscript received November 29, 2018. Published January 2, 2019. *This paper is part of the JES Focus Issue of Selected Papers from IMLB 2018.*

The development of reliable high energy density rechargeable Li ion batteries and their world-wide commercialization can be considered as the most important and impressive success of modern electrochemistry. The success of this battery technology promotes in these days the electro-mobility revolution. The Li batteries community gain experience and self confidence that enable it to suggest development of batteries with very high energy density comprising Li metal anodes^{1,2} and very high specific capacity cathodes like sulfur^{3,4} and oxygen.⁵ In fact, intensive work was devoted to rechargeable Li metal anode batteries during the eighties^{6,7} and the nineties⁸⁻¹³ of the previous century, including attempts to commercialize several secondary Li metal batteries.^{14,15} Due to discovery of intrinsic problems related to the stability of liquid electrolyte solutions in rechargeable Li metal batteries, safety consideration and the success of Li ion battery technology that seemed to rival Li metal based batteries, work in Li metal anodes for rechargeable batteries was mostly abandoned around the years 2000–2005.¹⁶ Since then, the batteries community gained a lot of new insights that led to a renaissance in developing again rechargeable battery systems comprising Li metal anodes in recent years.^{1,2,17-20} A lot of efforts in these days are devoted to developing solid state secondary Li batteries.^{21,22} In this paper we intend to discuss battery prototype systems with Li metal anodes and liquid electrolyte solutions, because of their advantages related to high rate capability and a possibility to operate them even at very low temperatures.²³ During the last decade we have been working intensively in the field of Li-oxygen batteries and discovered too many intrinsic problems related to the cathode side⁵ (even if the problems related to the Li anodes can be mitigated by appropriate protection strategies).²⁴⁻³⁰

It appears that all non-aqueous electrolyte solutions that can be relevant to Li-oxygen cells are reactive with the Li superoxide and peroxide species formed in solution phase upon oxygen reduction.³¹⁻³³ Thereby, the existence of detrimental side reactions in these systems seems to be unavoidable.³⁴⁻³⁵ Turning to the other high energy density systems, namely, Li-sulfur batteries, they suffer from well-known problem of a shuttle mechanism between the Li anode and the LiS_n sulfur reduction products which avoid their full recharge ability and

hence limit the practical specific capacity of the sulfur cathodes.^{36,37} It seems however that the shuttle mechanism problem can be solved.³⁸⁻⁴¹ Indeed, an impressive progress is recorded in developing some Li-S systems which may found practical uses.⁴¹⁻⁴⁵ These systems are not discussed further herein. The most relevant power sources for electro-mobility are high energy density Li ion batteries, which energy density is determined by the Li intercalation cathodes used.^{46,47} The most promising cathodes for Li ion batteries belong to the NCM family – $\text{Li}_{1+x}\text{Ni}_y\text{Co}_z\text{Mn}_w\text{O}_2$, which can be divided into 2 sub-groups of compounds: When $x>0$ and $w>0.5$ the cathode materials are defined as Li and Mn rich compounds (not discussed in this paper). More important seem to be the so called Ni rich cathode materials ($x = 0$, $y>0.5$) as discussed further in the core of the paper.

This paper is both a review and a perspective article that matches the purpose of the IMLB 2018 focus issue. After extensive recent work on Li – $\text{Ni}_{0.6}\text{Co}_{0.2}\text{Mn}_{0.2}\text{O}_2$ cells, Li – LiNiO_2 cells and graphite – LiMn_2O_4 (LMO) cells (the latter containing functional separators), we reached important integral view-points which led us to new insights about capacity fading and relatively simple stabilization mechanisms for the Ni rich NCM cathodes. Parallel intensive work on graphite – LMO cells which capacity fading could be remarkably mitigated by the use of functional separators, enables to suggest LMO as an important cathode material for long term applications. We discuss herein new perspectives that one can gain by reviewing rigorously our recent work.

Experimental

Li-metal foils with a thickness of 0.25 mm (Rockwood Lithium or FMC Chemicals Limited) that were kept in an argon-filled glove box were used without any pretreatment. Stoichiometric LiNiO_2 was synthesized using spherical $\text{Ni}(\text{OH})_2$ and $\text{LiOH} \cdot \text{H}_2\text{O}$ precursors mixed with molar ratio $\text{Li}/\text{Ni} = 1.01:1$ and calcined at 650°C for 10 h under an oxygen atmosphere. Detailed description of the synthesis is presented in Ref. 48. For composite electrodes preparation LiNiO_2 powder was mixed with conducting agent and poly(vinylidene fluoride) in a weight ratio of 90:5.5:4.5 in N-methylpyrrolidinone. The conducting agent was a mixture of graphite KS-6 and carbon black in a weight ratio of 6: 4. The slurry was spread onto Al foil, dried,

*Electrochemical Society Fellow.

**Electrochemical Society Member.

^zE-mail: Doron.Aurbach@biu.ac.il

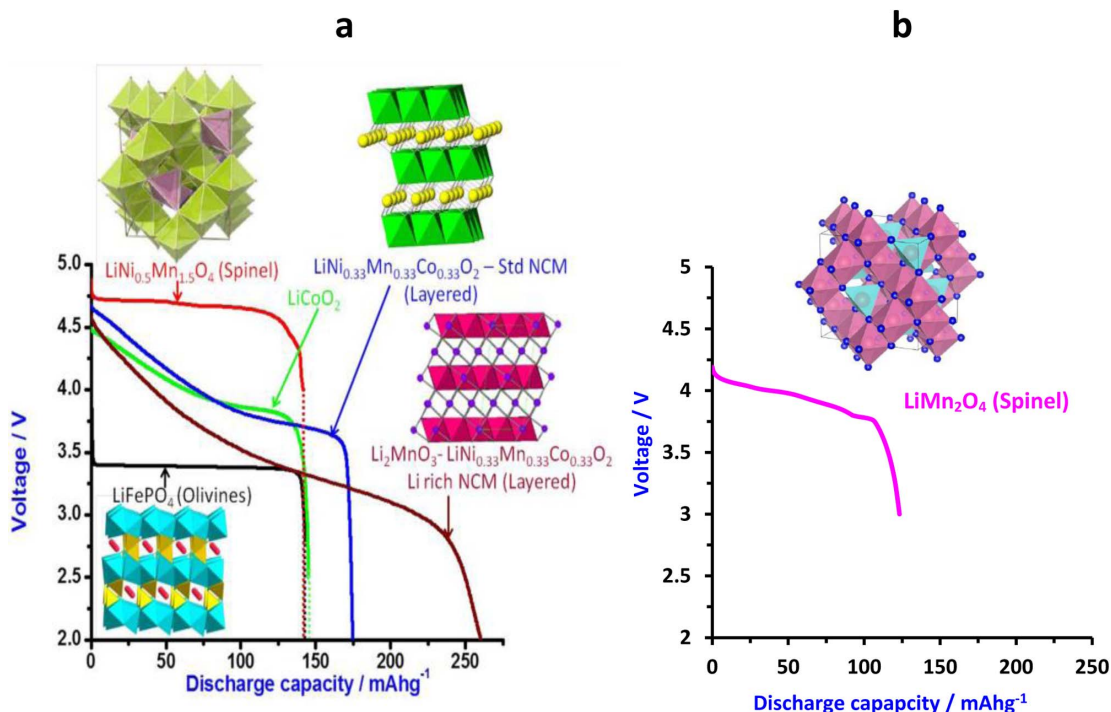


Figure 1. Li-ion battery cathodes: important formulae, structures and voltage profiles during discharge. The potentials are versus Li reference electrodes. (a) Reproduced with permission from Ref. 50. Copyright Elsevier 2014.

and roll-pressed. Cathode sheets comprising NCM 622 with the areal capacity of 3.3 mAh cm⁻² were obtained from BASF (Germany).

For galvanostatic tests, Li-metal foil electrodes 14 mm in diameter were assembled in two-electrode symmetric cell configurations using coin-type cells (2325, NRC, Canada). The electrolyte solutions were 1 M LiPF₆ in FEC/DMC 1:4, 1 M LiPF₆ in EC/DMC (Merck, Germany) and 1M LiTFSI/DOL/DME/LiNO₃. The amount of the electrolyte solution used was 50 μL/cell. With FEC-based and ethereal electrolyte solutions we used 2 layers of polyethylene (PE) separator (Tonen). With EC-based electrolyte solution polypropylene (PP) separator (Celgard) was used.

For galvanostatic tests of Li|LiNiO₂ and Li| NCM 622 cells Li-metal foil disk electrodes (thickness 0.25 mm, diameter 14 mm) and LiNiO₂ cathodes (27 mg of active material, diameter 14 mm) or NCM 622 cathodes (diameter 14 mm) were assembled in two-electrode configurations using coin-type cells (2325, NRC, Canada). The amount of the electrolyte solution used was 33 μL cm⁻² of electrodes (1.2 μL mg⁻¹ active material). Li| LiNiO₂ cells were cycled with a current density of 0.4–1.6 mA cm⁻² and cutoff voltage 2.8–4.3 V, and Li| NCM 622 cells were cycled with a current density of 0.5–2 mA cm⁻² between 2.8–4.3 V.

SEM images were obtained with Environmental Scanning Electron Microscope, Ouanta FEG 250 (FEI). Air sensitive samples were transferred from the Ar filled glove box to the chamber of the microscope with the use of homemade vacuum tight transferring cell.⁴⁹

The impedance spectra in the frequency range of 100 kHz–10 mHz (EIS) were measured using a potentiostat-galvanostat Model 128N Autolab (Eco Chemie).

X-ray diffraction (XRD) patterns were obtained with a D8 Advance system (Bruker Inc.) using Cu Kα radiation operated at 40 mA and 40 kV.

Results and Discussion

On the choice of cathode materials for Li batteries for electromobility applications.—Fig. 1 provides typical voltage profiles of the most important cathode materials and the basic crystal structure of the three main families of compounds: layered, spinel and olivine.

Since this is a review article, we emphasize herein briefly two important cathode materials that are beyond the scope of main work to which this paper relates. The first one is LiMn_{1.5}Ni_{0.5}O₄ spinel, whose redox potential (due to transition of Ni²⁺ to Ni⁴⁺) is around 4.8 V versus Li, with a flat potential profile (due to 2-phase transition reactions) but a limited capacity up to 147 mAh/g theoretically.⁵⁰ This cathode material is intrinsically highly stable and due to its spinel structure, it allows the 3D diffusion process of Li ions intercalation into it. As such, this cathode material exhibits excellent rate capability.^{51,52} In fact, there is another interesting high voltage cathode material, namely LiCoPO₄, whose redox potential (also via a 2-phase transition reaction) is around 4.8 V. However, this material suffers from intrinsic stability problems that are reflected in a relatively low specific capacity <120 mAh/g (versus 165 mAh/g theoretical) and capacity fading during prolonged cycling.⁵³

Another important cathode material presented in Fig. 1a is the family of Li- and Mn-rich layered cathode materials, discovered and developed a few years ago by Argonne National Lab (ANL) and other groups.⁵⁴ Preparation of lithiated mixed transition metal oxides, comprising the elements Li, Mn, Ni, O or Li, Mn, Ni, Co, O with an excess of Li and Mn, produces a pristine cathode material which contains two phases, Li₂MnO₃ (inactive) and Li[MnNi]O₂ or Li[MnNiCo]O₂ (active) mixed together on a nanometric scale. Polarization of these materials to potentials of >4.6 V versus Li leads to pronounced changes, including some release of oxygen and de-lithiation that activates the entire material and makes it fairly active. Here, the capacities may approach the maximal values for LiMO₂ stoichiometry (one e⁻ and one Li⁺ per MO₂) up to 300 mAh/g.

There is a great challenge in finding ways to stabilize these materials and thus benefit from intercalation cathode materials with a specific capacity close to the maximum around 300 mAh/g. A most important possible direction is coating, using particles with a core shell structure and a selection of compositions that provide better stability on the account of some specific capacity.^{55–57} More important than these Li and Mn rich NCM cathode materials are the Ni rich LiNi_xCo_yMn_{1-x-y}O₂ (x → 1) materials, i.e., Ni-rich NCM. Here a major advantage is the possibility to extract high specific capacity (> 200 mAh/g).⁵⁸ The higher the Ni content in these materials, the

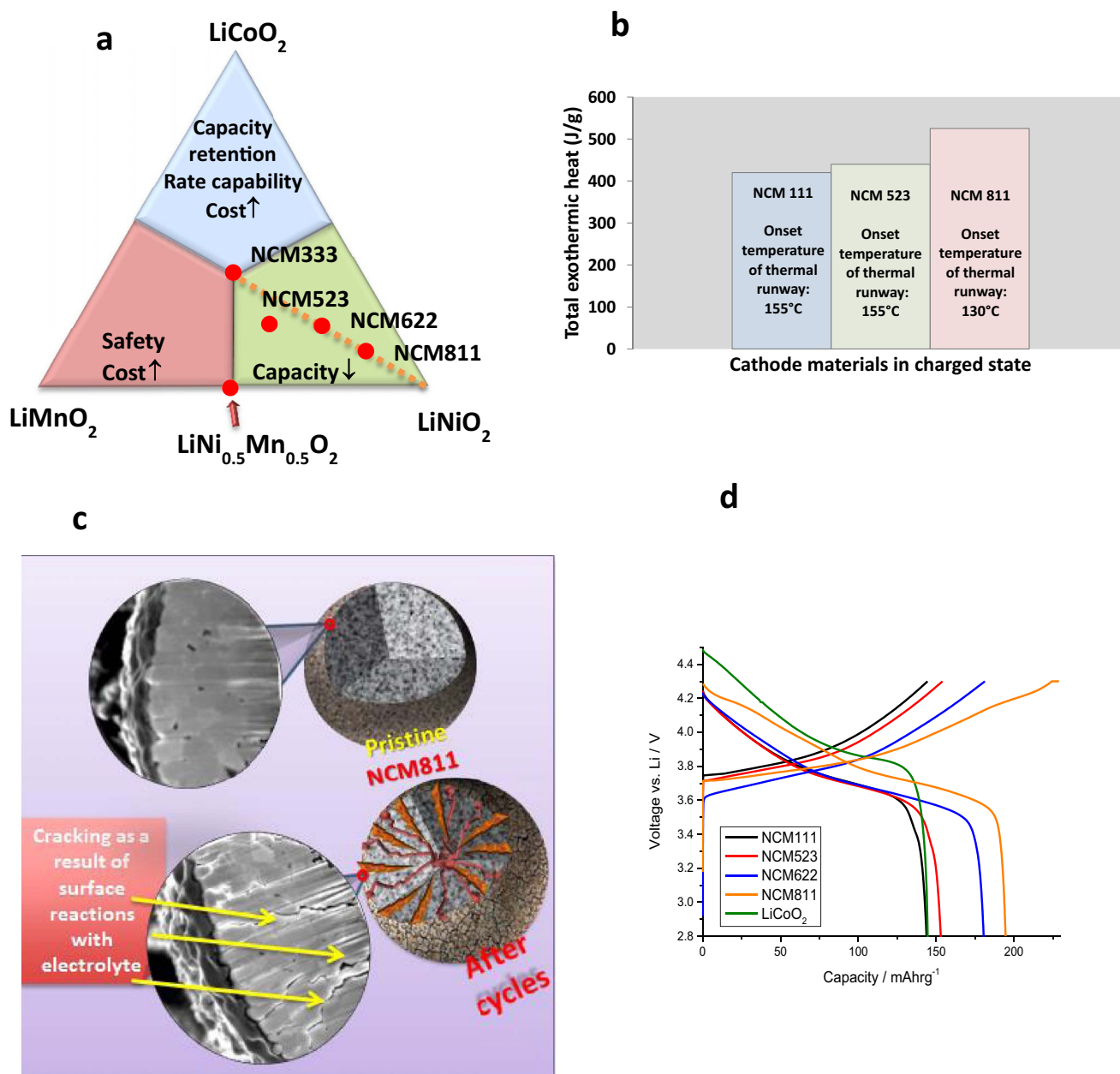


Figure 2. The effect of Ni content on the performance and properties of Ni-rich cathode materials. (a) Compositional phase diagrams of NCM layered oxide materials, (b) Thermal response of multi-layer pouch cells containing NCM cathodes, graphite anodes and 1M LiPF $_6$ in EC:EMC 3:7 + 2% VC, (c) Cross-sectional SEM view of cracks formed due to cycling of NCM 811, (d) Voltage profiles of NCM layered oxide cathodes and LiCoO $_2$ (a) Reproduced with permission from Ref. 66, Copyright 2018, Wiley-VCH. (c) Adopted from Ref. 61 and with permission from Ref. 66. Copyright 2018, Wiley-VCH.

higher its specific capacity, up to a 240 mAh g $^{-1}$ limit posed by LiNiO $_2$ (LNO).⁵⁹ The clear advantage of Ni-rich NCM is the high capacity that can be extracted with charging potentials below 4.3 V versus Li/Li $^+$.⁵⁵ LIB with such cathodes can thus be fully charged without reaching potentials that impair the stability of LiPF $_6$ /carbonates electrolyte solutions. However, due to their higher Ni content, these materials are more sensitive both mechanically (fatigue cracking upon prolonged cycling) and electrochemically (more reactive in side reactions with the electrolyte solutions).^{60–62} Fig. 2a shows the phase diagrams of three individual lithiated oxides LiNiO $_2$, LiCoO $_2$, LiMnO $_2$ with various compositions of Ni, Co, and Mn. Although Ni-rich NCM cathode materials offer high capacity as shown in the green area of Fig. 2a, further improvements and optimization are needed in order to realize their full potential as cathode materials for LIBs. The three transition metal ions in the NCM cathodes have specific functions in terms of

their structure and electrochemical performance, which enable them to be used as effective Li insertion electrodes. The Ni $^{2+/3+}$ and Ni $^{3+/4+}$ redox couples provide the majority of the reversible capacity. Thermal response of multi-layer pouch cells containing NCM cathodes, graphite anodes and electrolyte presented in Fig. 2b gives an indication of a lower thermal stability of NCM cathodes with higher Ni content. Fig. 3d shows typical voltage profiles of these cathodes, demonstrating the effect of Ni content on their specific capacity. Apart from the layered ordering, the presence of cobalt improves the rate performance, in addition to the capacity obtained from the Co $^{3+/4+}$ redox reaction. The presence of Mn stabilizes the local structure, and Mn $^{4+}$ remains electrochemically inactive during cycling. Four problems are exacerbated with the increase in Ni content: i) cation mixing between Li and transition metals during synthesis, mainly Li $^+$ /Ni $^{2+}$, which interferes with the mobility of Li ions; ii) low thermal stability

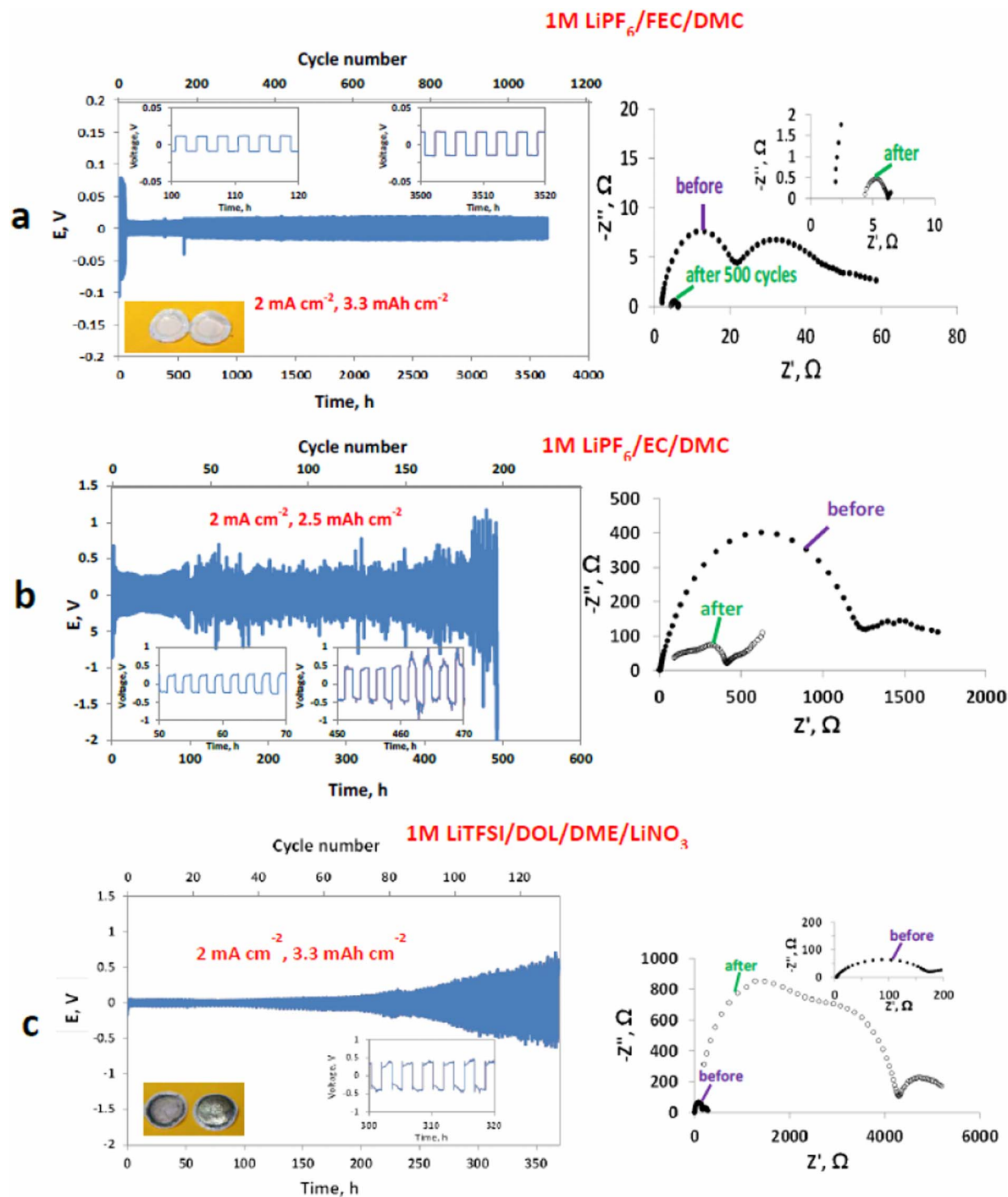


Figure 3. Galvanostatic cycling results and Nyquist plots measured for symmetric Li|Li cells before (full dots) and after cycling (hollow dots). Insets: images of cycled separators. Electrolyte solutions (a) 1M LiPF₆/FEC/DMC, (b) 1M LiPF₆/EC/DMC, (c) 1M LiTFSI/DOL/DME/LiNO₃ (33 μL cm⁻²). Reproduced with permission from Ref. 49. Copyright 2017, American Chemical Society.

(Fig. 2b); iii) formation of cracks during prolonged cycling (Fig. 2c); and iv) surface reactivity.⁶³⁻⁶⁶ Since in this paper we intend to discuss insights from testing Li-LiNO₂ cells, it is important to mention some recent work on Li anodes.

Reconsideration of Li metal anodes for high energy density Li batteries.—In our recent works we demonstrated a very stable Li metal stripping—plating at a high rate and high areal capacity in FEC-based electrolyte solution.^{49,67} Typical galvanostatic cycling results

obtained for three Li|Li cells cycled in three important electrolyte solutions with areal charge/discharge capacity of 2.5–3.3 mAh/cm² and current density of 2 mA cm⁻² are shown in Fig. 3. The cells cycled in the FEC-based electrolyte solution (Fig. 3a) demonstrates stable behavior for more than 3600 hours (more than 1100 cycles) with a voltage profile typical for a stable and homogeneous lithium plating/stripping process.^{68,69} For the cells with FEC-based electrolyte solution after the initial cycling with higher voltage profiles we always observed stabilization with lower voltage profiles. This behavior is

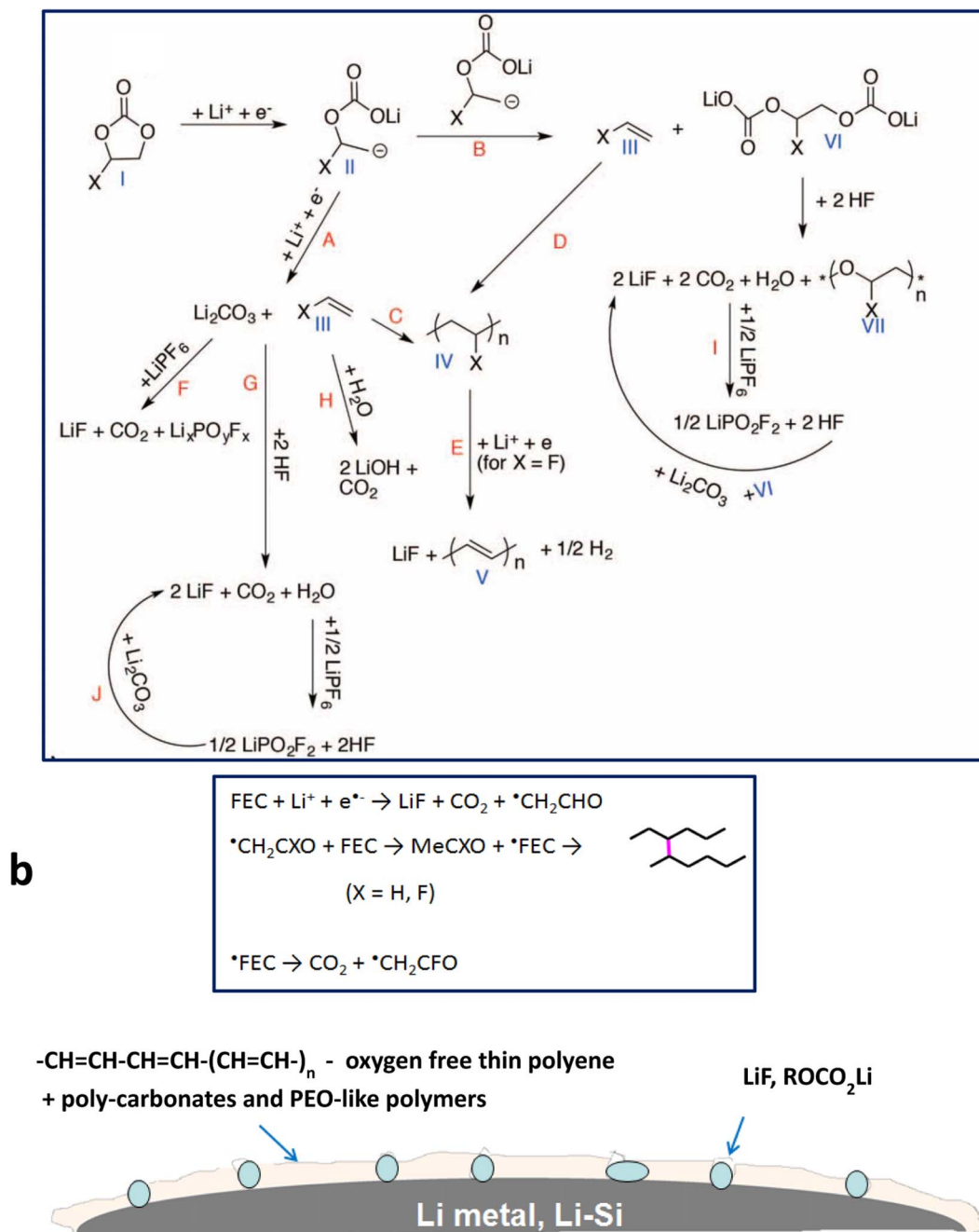


Figure 4. Possible surface reactions of FEC based solutions with LiPF₆ on Si electrodes. FEC reduction forms flexible polymeric matrices based on polyolefins, in which LiF is embedded, serving as Li ions conductors. Such films accommodate better the volume changes of these electrodes. Reaction scheme proposed in Ref. 71 (a) and in Ref. 73, 74 (b). (c) A depiction of polymer film developed on Si or Li metal anodes from FEC-based solutions. (a) Reproduced from Ref. 71, (b) Adopted with permission from Ref. 74. Copyright 2015, American Chemical Society.

well known and relates to the reorganization of the Li surface (increasing of surface area) and the formation protective surface films, which maintain prolonged cycling of the high specific surface area Li electrodes.⁷⁰

Cells cycled with the same current density in EC-based electrolyte solutions (standard ones for Li ion batteries) demonstrate a much higher and more unstable voltage during both charge and discharge steps and fail after about 200 cycles (Fig. 3b). In ethereal solutions (commonly used in Li-S batteries) the cells typically performed only 100–200 cycles before failure and demonstrate monotonically increasing in the voltage profile due to dendrites formation and the depletion of the electrolyte solution (Fig. 3c). Thus, typically the

symmetric Li|Li cell cycled with the FEC based electrolyte solution shows markedly better cycling behavior than that observed for the cells cycled with the EC-based and ethereal electrolyte solutions.

The cell cycled in the FEC-based electrolyte solution was stopped and disassembled after 1100 cycles of stable cycling. The separator was wet indicating that no massive dendrite formation accompanied by the depletion of the electrolyte occurred in this case. To the contrary, all the separators from the cells cycled in the EC-based and ethereal solutions disassembled after 200 and 130 cycles, respectively, were dry. The insets in Figs. 3a and 3c present the images of Li anodes and PE separators after cycling. It is clearly seen that for the FEC based solution the inner sides of separators after cycling are free of

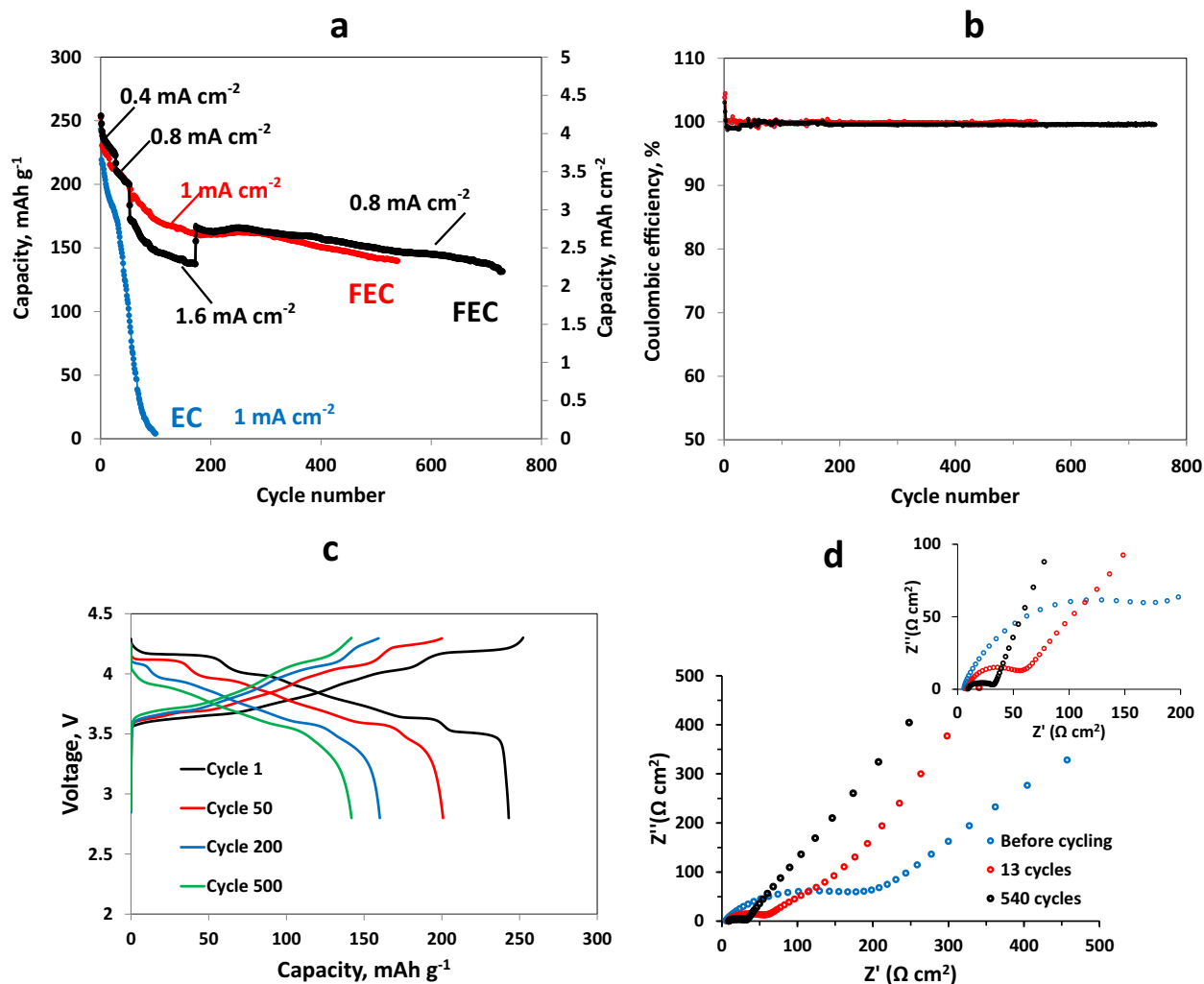


Figure 5. (a) Cycling performance of Li|LiNiO₂ cells cycled in FEC-based electrolyte solution with current densities as indicated (red and black curves) and EC-based electrolyte solution (blue curve). (b) Coulombic efficiency of Li|LiNiO₂ cells (c) Voltage profile measured for Li|LiNiO₂ cells cycled with a current density 1 mA/cm². (c) Nyquist plots measured at 3.0V for Li|NMC cells before cycling, after 13 cycles and after 540 cycles, as indicated. The 1st cycle was performed with a current density of 0.12 mA/cm² and the 2nd – at 0.24 mA/cm². Diameter of electrodes 14 mm. The amount of the electrolyte solution 33 μl cm⁻². 30°C. Reproduced with permission from Ref. 80. Copyright 2018, American Chemical Society.

metallic Li and preserve their integrity. In contrast, after cycling in the ethereal solution Li was accumulated between 2 separators due to the penetration of Li dendrites through the separators.

Typical Nyquist plots measured for symmetric Li|Li cell before and after cycling are presented in Fig. 3. A drastic decrease in the surface film and charge transfer resistances of the cells cycled in the FEC-based solution implies the changes in the morphology of Li metal anodes with an increase of the effective surface area of the electrodes.⁶⁸ For the cell with EC-based solution very high impedance before cycling is obviously caused by slow diffusion of Li ions in the pores of PP separator due to its poor wettability in this electrolyte solution. After cycling the failed cell demonstrates much higher impedance than that of the cell cycled in the FEC-based solution. A huge impedance of the cell failed in the ethereal solution is indicative for the depletion of the electrolyte and drying due to massive dendrite formation.

Thus, excellent cycling performance of Li metal anodes was demonstrated in the EC-free FEC-based organic carbonate electrolyte. Symmetric Li|Li cells demonstrated an extremely long cycle life and stable voltage profile for more than 1100 cycles at a current density of 2 mA cm⁻² and areal capacity of 3.3 mA h cm⁻² with minimal amount of the electrolyte solution sufficient for wetting of the separator in the coin cells (50 μL/cell). High performance of Li anodes we attribute

to the formation of stable and efficient SEI on the surface of the Li metal electrodes cycled in the FEC-based electrolyte solution.

The surface chemistry developed on Li-metal and Si negative electrodes in FEC based solutions was thoroughly explored by our group. Fig. 4a presents the reduction reactions of FEC in the presence of Li⁺ detected on lithiated Si anodes. According to XPS data oxygen free carbon containing species are the main components of the surface films which are formed on Si anodes in FEC-based electrolyte solution and unsaturated polymer V is the most important component for the effective passivation of Si anode surfaces.^{71,72} The formation of the unsaturated polymer film on the surface of Si anodes prevents further decomposition of the electrolyte solution and further formation of carbonate surface species. A very similar XPS spectra measured from Li metal anodes in symmetric Li|Li cells suggests that the reactions presented in Fig. 4a take place on the surface of Li anodes as well. The other components found on the surface of Li metal anodes are polycarbonates and PEO-like polymers.⁶⁷

Another possible reaction path of FEC transformation on Si anodes presented in Fig. 4b relate to •CH₂CHO and •CH₂CFO radicals that can abstract H from FEC, initiating chain reactions which lead finally to the formation of oxygen free cross-linked polymers on the electrodes' surfaces.^{73,74} While most of the surface analytical work we

carried out on FEC based solutions was with lithiated silicon anodes, the conclusions seems to be relevant to Li metal anodes as well.

A depiction of polymer films developed on Si or Li metal anodes from FEC-based solutions is shown in Fig. 4b. The reduction reactions of FEC in the presence of Li^+ lead to the formation of polymeric species (elastomeric components) and LiF clusters. The latter serve as SEI components that allow free Li^+ migration through these surface films.

High energy density Li batteries based on high specific capacity Ni-rich cathodes and Li metal anodes.—Due to effective passivation of the surface of anodes by the formation of thin elastic surface films in FEC-based electrolyte solution we achieved an excellent cycling performance of Li metal anodes in symmetric Li|Li cells with commercial current density and areal capacity. It is very important, however, to achieve stable long-term operation of full Li|cathode cells with a practical level of energy density per unit area. The unique properties of FEC which forms effective protective SEI on both anodes (as discussed above) and cathodes^{75,76} make it an excellent component in electrolyte solutions for Li batteries. We showed that FEC based electrolyte solution significantly improves the cycling performance of cathodes including 5V $\text{LiNi}_{0.5}\text{Mn}_{1.5}\text{O}_4$ spinel cathodes,⁷⁷ high capacity integrated $x\text{Li}_2\text{MnO}_3 \cdot (1-x)\text{LiNi}_y\text{Mn}_z\text{Co}_{1-y-z}\text{O}_2$ cathodes⁷⁸ and even 5 V LiCoPO_4 cathodes, which are very problematic.^{53,79} In our recent works we demonstrated a very stable cycling performance of Li|NCM 622 and Li|LiNiO₂ cells with practical loading of cathode material and low amount of FEC-based electrolyte solution.^{49,67,80}

Galvanostatic cycling results obtained for Li|LiNiO₂ cells with areal charge/discharge capacity of about 4 mAh cm^{-2} cycled in FEC-based electrolyte solution are shown in Fig. 5a. A very stable cycling of the cells with about 100% efficiency for 540 cycles was observed at a current density of 1 mA cm^{-2} (Figs. 5a, 5b red curves). The cells demonstrated voltage profiles typical for LiNiO₂ cathodes (Fig. 5c). The black curves shown in Fig. 5a relate to the cells cycled with different current densities and reflect a very good rate capability of LiNiO₂ cathodes with high areal loading. The cells underwent more than 700 cycles without pronounced capacity fading. A moderate capacity fading observed up to about 150 cycles was followed by stabilization with very low capacity loss per cycle. The blue curve in Fig. 5a demonstrates cycling performance of Li|LiNiO₂ cells with EC-based electrolyte solutions. It is seen that FEC-based solution significantly outperforms EC-based solution. Obviously, FEC provides more effective stabilization for both the cathodes and the anodes in Li batteries due to the formation of more effective protective surface films.⁸⁰ The significantly higher Coulombic efficiency that was measured for Li|Cu cells with FEC-based compared to EC-based electrolyte solution supports this conclusion.⁶⁷ Typical Nyquist plots measured with Li|LiNiO₂ cells before cycling and after 13 and 540 cycles are presented in Figure 5d. The decrease in the surface films and charge-transfer related resistances of the cells reflected by the impedance spectra due to cycling is obviously relates to the changes in the morphology of the Li metal electrodes with increase in the effective surface area of the Li anodes, since the LiNiO₂ cathodes do not change pronouncedly during cycling.^{67,80}

SEM images of the pristine LiNiO₂ material are shown in Figs. 6a, 6c, 6e and LiNiO₂ cathodes cycled in a Li|LiNiO₂ cell for 540 cycles are presented in Figs. 6b, 6d, 6f. It is seen that LiNiO₂ particles remained undamaged without any signs for micro-cracks formation. We could not observe cathodes' particles with visible damages after prolonged cycling. Typical particles related to cycled cathodes (Fig. 6f) are almost indistinguishable in their morphology from that of the pristine LNO material (Fig. 6e). XRD patterns of cycled LiNiO₂ cathodes presented in Fig. 6g did not reveal the formation of new phases, as well as the ratio of the intensities of the peaks remained unchanged. These observations confirm structural stability of the LNO electrodes during prolonged cycling.

The scheme of the formation of surface films on the surface of LiNiO₂ particles in EC and FEC based electrolyte solutions and de-

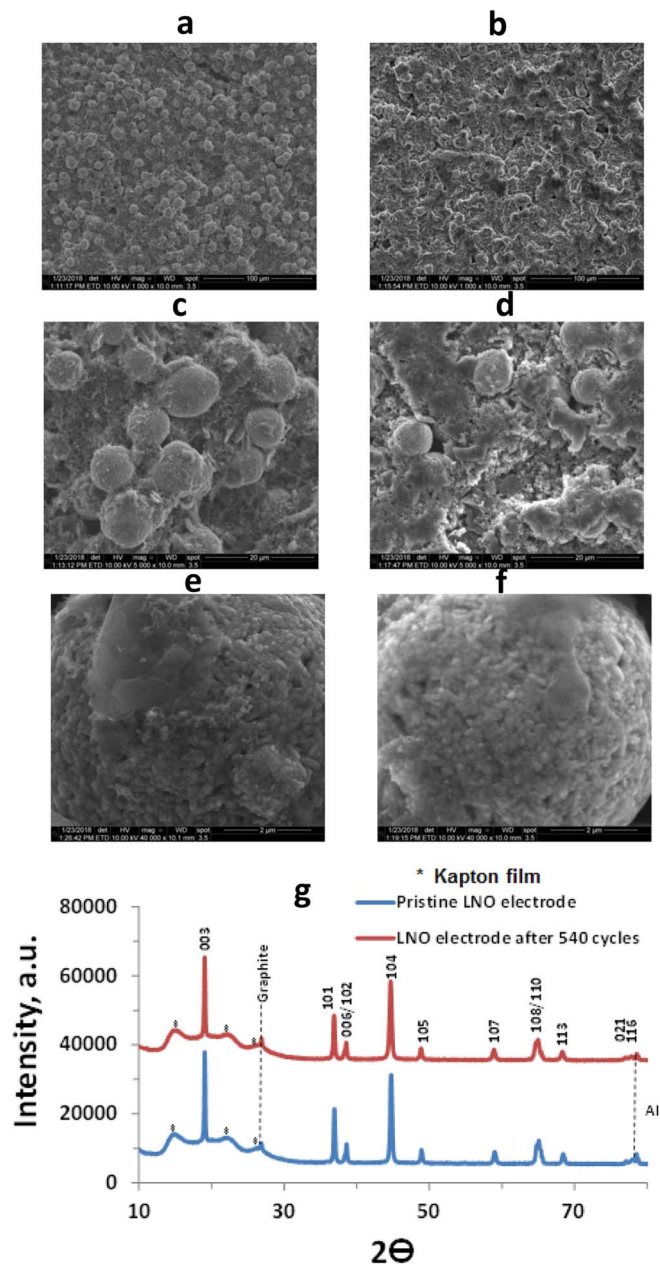


Figure 6. SEM images of pristine LiNiO₂ cathode (a, c, e) and LiNiO₂ cathode cycled in Li|LiNiO₂ cell for 540 cycles (b, d, f) at different magnifications and XRD patterns of pristine LiNiO₂ electrodes and LiNiO₂ electrodes in fully lithiated state from Li|LiNiO₂ cell after 540 cycles with a current density of 1 mA cm^{-2} in 1M LiPF_6 FEC/DMC electrolyte solution (g). Peaks marked with asterisks relate to Kapton film. Reproduced with permission from Ref. 80. Copyright 2018, American Chemical Society.

velopment of cracks in the secondary LiNiO₂ particles during cycling in EC-based electrolyte solutions is presented in Fig. 7a. It is remarkable that with FEC-based electrolyte solutions, very stable cycling behavior of LiNiO₂ cathodes was observed during cycling in a full potential range of 2.8–4.3 V (Fig. 5), whereas in Ref. 48 (Fig. 7b) it was shown that cycling LiNiO₂ cathodes with upper cutoff voltage higher than 4.1 V led to capacity loss because of structural damage due to $\text{H}_2 \rightarrow \text{H}_3$ phase transition accompanied by micro-cracking. Capacity fading of LiNiO₂ is associated with phase transformations at high states-of-charge and surface instability.^{48,62,81,82} According to Refs. 65,83–86 the formation and propagation of micro-cracks upon cycling arises from the anisotropic lattice volume changes, which

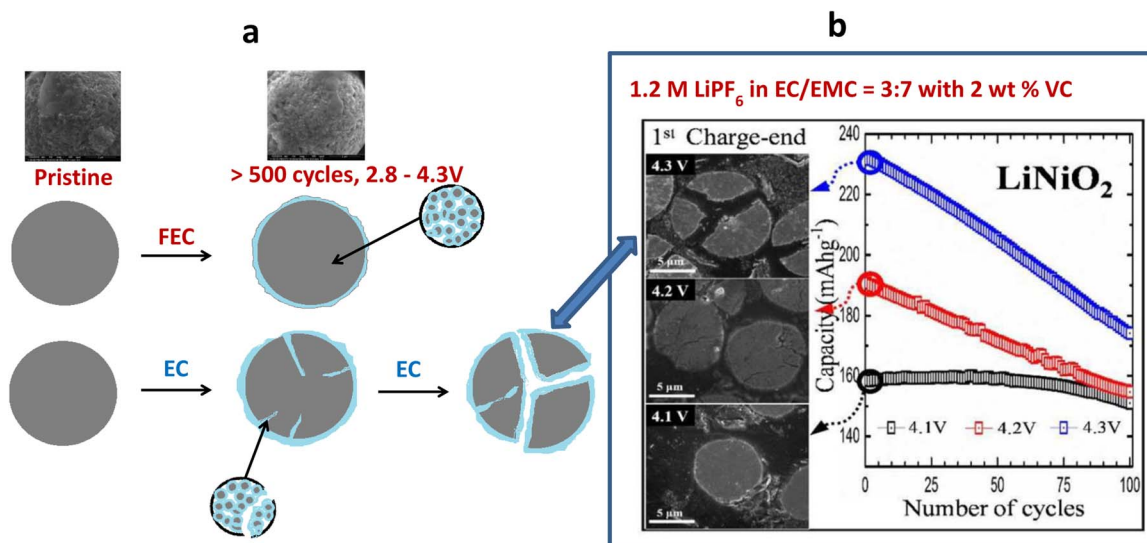


Figure 7. (a) Schematic presentation of the formation of surface films on the surface of LiNiO₂ particles in EC and FEC based electrolyte solutions and development of cracks in the secondary LiNiO₂ particles cathode during cycling in EC-based electrolyte solution. (b) Cross-sectional SEM images of the initial charge-ended LiNiO₂ cathodes and cycling performance of LiNiO₂ cathodes at different upper cutoff voltages, as indicated. (b) Reproduced with permission from Ref. 48. Copyright 2017, American Chemical Society.

lead to grain separation and intensive reactions of the active mass with components of the electrolyte solutions used in Li ion batteries. Besides, it is known that chemical and electrochemical reactions of the lithiated transition metal oxide cathode materials with components of the standard electrolyte solutions used in Li batteries cause degradation of the cathode surface.^{87,88} Such surface reactions accompanied by electrolyte solution decomposition and gas generation deteriorate the performance of Li batteries. The problem of gas evolution is especially important for Ni-rich materials, as the increase of Ni content in the cathode increases also the amount of LiOH and Li₂CO₃ residues on the particles. LiOH reacts nucleophilically with alkyl carbonates while Li₂CO₃ decomposes to form CO₂ gas.⁸⁹ Due to unavoidable strains and stresses developed in the particles during repeated Li insertion/de-insertion cycling, micro-cracks are formed in them. In the absence of effective passivation, electrolyte solution can penetrate into the cathode particles through the micro-cracks formed during cycling, reacting with a fresh cathode material, thereby expediting the degradation of the cathode's active mass.^{83,84,90-93} In Ref. 80 it was shown by XPS that the main components which are formed on the surface of LNO cathodes after cycling in FEC-based electrolyte solutions are LiF, as well as C- and O-containing substances, including Li₂CO₃, Li alkyl carbonates and polyethylene oxide (PEO)-like polymer species. Thus, the choice of electrolyte solutions which induce favorable surface chemistry is very important to attain stable

cycling of cathodes comprising the very reactive LiNiO₂. Obviously, an excellent stability of high capacity stoichiometric LiNiO₂ cathodes in FEC-based electrolyte solutions is achieved due to the formation of effective protective surface films.

Another example of excellent cycling stability of Ni-rich cathodes with practical loading in Li|NCM 622 cells with Li metal anodes in FEC-based electrolyte solutions is shown in Fig. 8. The cells with electrodes' loading of 3.3 mA h g⁻¹ can undergo many hundreds of stable cycles, demonstrating high rate capability. It is remarkable, that Li|NCM 622 cells can be cycled at 1.5 mA cm⁻² for more than 600 cycles, whereas symmetric Li|Li cells demonstrate stable performance for more than 1000 cycles even at higher areal capacity and current density (Fig. 3a).^{49,67} In a follow up work, EMC:FEC based electrolyte solutions were also found to be very suitable for Li-NMC 622 and Li-LNO cells with practical loading (around 2 and 5 mAh/cm² respectively).⁹⁴ That work is a further substantiation of the importance of FEC as an excellent co-solvent for high energy density secondary Li (metal) batteries, as we discovered in the work described herein.

According to spectroscopic studies of solutions from cycled cells by NMR measurements,⁶⁷ cycling Li|NCM is accompanied by a much faster consumption of FEC compared to the situation in symmetric Li|Li cells. The performance of the full cells strongly depends on the current density and the amount of the electrolyte solution in them. We attribute this observation to the involvement of the products of

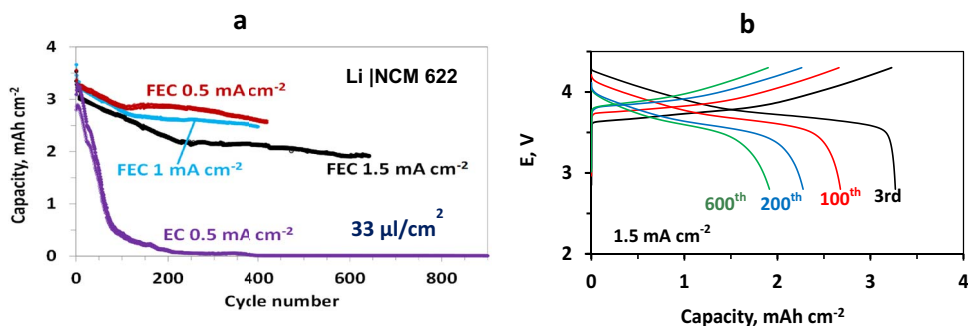


Figure 8. (a) Galvanostatic cycling results obtained for Li|NCM cells cycled with different current densities, as indicated, in FEC and EC based electrolyte solutions and (b) voltage profile measured for Li|NMC cells cycled with a current density 1.5 mA/cm² in FEC based electrolyte solution. The amount of electrolyte solution used was 33 μL/cm². Adopted with permission from Ref. 67. Copyright 2018, American Chemical Society.

the oxidative decomposition of the electrolyte solution at the positive electrodes in detrimental side reactions on the Li anodes, which worsen their passivation. These products are transferred further to the anodes being reduced on the anodes to form solid and gaseous products, which were detected by XPS and FTIR. These side processes lead both to a faster depletion of the electrolyte solution in the cycled cells and to the growth of resistive surface films on the Li anodes, resulting in kinetics problems. According to the XPS measurements, the content of LiF in the surface films on Li anodes, which are formed in Li|NCM cells, is markedly higher than that formed in symmetric Li|Li cells.

Even though full Li|NCM cells demonstrated a lower cycling stability than symmetric Li|Li cells, in Ref. 67. We unambiguously and strongly substantiated conclusions about the unique properties of solutions containing FEC as a co-solvent on the stability of all kinds of rechargeable Li cells containing Li metal anodes. The most important insight obtained from the studies reviewed herein relate to a better understanding of the degradation and stabilization mechanisms of Ni rich NCM cathodes. Extensive work was devoted to doping NCM cathode materials as a mean for their stabilization, via mitigation of strains, stresses and cracking.^{66,95,96} A specially interesting example is our recent studies on W doped LNO electrodes that revealed a complex behavior of the doped cathode material. These electrodes demonstrate a stable performance due to complicated bulk and surface rearrangements.⁹⁷ In turn, our results show that much simpler means, related to simple surface protection, can reach impressive stabilization of these sensitive materials. Our results mean that high energy density Li ion cells based on very high specific capacity LNO cathodes can be fabricated, thus fulfilling the needs of high energy density batteries for EV applications.

Abundance of metals and alternative cathodes for future needs of electric vehicles, if the electro-mobility revolution will succeed.—

Since the massive use of batteries based on Ni rich NCM cathodes for electro-mobility seems to be very realistic, it is important to discuss the availability of nickel as a major component in them, taking into account that recycling of used batteries will not meet the demands of new batteries, if EVs will conquer the roads all over the world. Although the authors of recently published works claim that according to their calculations nickel has sufficient supply to meet the increase in demand for Li batteries,^{98,99} it can be clearly anticipate that a success of the electro-mobility revolution will obviously lead to a shortage of nickel. Hence, in order to promote long term use of EVs on the roads we have to suggest batteries that use more abundant materials than nickel. Manganese is much more abundant than nickel in earth crust.^{100,101} We can suggest LiMn₂O₄ (LMO) cathodes for EV batteries when we will reach a shortage in nickel. Using LMO cathodes means a compromise on energy density (Fig. 1b) but a pronounced gain in rate capability, better low temperature performance, cost and high round energy efficiency per cycle. In turn, the use of LMO cathodes in Li ions batteries introduces a severe durability problem due to the well-known issue of Mn ions dissolution from the cathodes into the electrolyte solutions. The presence of Mn ions in solutions in Li ion batteries is very detrimental for the passivation of the graphite anodes and hence for the stability of the cells during prolonged cycles. However, for this problem we developed a solution based on the use of relatively cheap and easy to prepare functional separators which trap Mn ions during the critical stage in which the passivation of the graphite anodes is built-up, during the first cycles of the cells.^{66,102,103} These developments can facilitate the use of LMO based Li ion cells for applications that require prolonged cycle-life.

Conclusions

This review article summarizes previous work related to symmetric Li|Li cells, and containing Li anodes and Ni rich NCM cathodes. The fact that electrolyte solutions containing FEC as a co-solvent passivates very well both Li metal anodes and Ni rich NCM cathodes enabled to test at practical rates Li-LNO and Li-NCM 622 cells

comprising electrodes with practical loading (3.3–4 mAh/cm²) during very prolonged cycling experiments. Usually, LiNiO₂ cathodes cycled with an upper potential limit up to 4.3 V vs. Li, suffers from pronounced capacity fading. We understand now the major mechanism: stresses related to the phase transitions that these cathodes undergo upon delithiation/lithiation cycles (up to 4.3 V) forms cracks that expose active Li_xNiO₂ area to solution species. The surface reactions within the cracks promote further propagation and intensification of cracking and detrimental side reactions which decompose the particles of the active mass.

This destruction mechanism can be mitigated by doping LNO with foreign multivalent cations such as W⁵⁺.⁹⁷ Our studies show that using electrolyte solutions containing FEC which anodic reactions cover the LNO particles by protective surface films, which remarkably mitigate capacity fading. Such surface films avoid contact between the active mass and solutions species. Hence, even if some cracking occurs during initial cycling, the cracks thus formed do not propagate further if the active mass is effectively isolated from the solution species by flexible SEI type surface films.

ORCID

Elena Markevich  <https://orcid.org/0000-0002-6851-0475>
 Gregory Salitra  <https://orcid.org/0000-0003-4309-4249>
 Doron Aurbach  <https://orcid.org/0000-0002-1151-546X>
 Yang-Kook Sun  <https://orcid.org/0000-0002-0117-0170>

References

1. X.-B. Cheng, R. Zhang, C.-Z. Zhao, and Q. Zhang, *Chem. Rev.*, **117**, 10403 (2017).
2. W. Xu, J. Wang, F. Ding, X. Chen, E. Nasybulin, Y. Zhangad, and J.-G. Zhang, *Energy Environ. Sci.*, **7**, 513 (2014).
3. A. Manthiram, Y. Fu, S.-H. Chung, C. Zu, and Y.-S. Su, *Chem. Rev.*, **114**, 11751 (2014).
4. A. Rosenman, E. Markevich, G. Salitra, D. Aurbach, A. Garsuch, and F. F. Chesneau, *Adv. Energy Mater.*, **5**, 1500212 (2015).
5. D. Aurbach, B. D. McCloskey, L. F. Nazar, and P. G. Bruce, *Nature Energy*, **1**, 16128 (2016).
6. K. M. Abraham, J. L. Goldman, and M. D. Dempsey, *J. Electrochem. Soc.*, **128**, 2493 (1981).
7. I. Yoshimatsu, T. Hirai, and J. Yamaki, *J. Electrochem. Soc.*, **135**, 2422 (1988).
8. D. Aurbach, Y. Gofer, and M. Ben-Zion, *J. Power Sources*, **39**, 163 (1992).
9. D. Aurbach, A. Zaban, A. Schechter, Y. Ein-Eli, E. Zinigrad, and B. Markovsky, *J. Electrochem. Soc.*, **142**, 2873 (1995).
10. D. Aurbach, Y. Gofer, M. Ben-Zion, and P. Aped, *J. Electroanal. Chem.*, **339**, 451 (1992).
11. D. Aurbach, M. Moshkovich, Y. Cohen, and A. Schechter, *Langmuir*, **15**, 2947 (1999).
12. D. Aurbach, O. Youngman, Y. Gofer, and A. Meitav, *Electrochim. Acta*, **35**, 625 (1990).
13. M. Moshkovich, Y. Gofer, and D. Aurbach, *J. Electrochem. Society*, **148**, E155 (2001).
14. D. Aurbach, I. Weissman, H. Yamin, and E. Elster, *J. Electrochem. Soc.*, **145**, 1421 (1998).
15. E. Mengeritsky, P. Dan, I. Weissman, A. Zaban, and D. Aurbach, *J. Electrochem. Soc.*, **143**, 2110 (1996).
16. D. Aurbach, E. Zinigrad, H. Teller, and P. Dan, *J. Electrochem. Soc.*, **147**, 1274 (2000).
17. F. Ding, W. Xu, G. L. Graff, J. Zhang, M. L. Sushko, X. Chen, Y. Shao, M. H. Engelhard, Z. Nie, Jie Xiao, X. Liu, P. V. Sushko, J. Liu, and J.-G. Zhang, *J. Am. Chem. Soc.*, **135**, 4450 (2013).
18. M.-H. Ryou, Y. M. Lee, Y. Lee, M. Winter, and P. Bieker, *Adv. Funct. Mater.*, **25**, 834 (2015).
19. J.-S. Kim, D. W. Kim, H. T. Jung, and J. W. Choi, *Chem. Mater.*, **27**, 2780 (2015).
20. Y. Liu, D. Lin, Z. Liang, J. Zhao, K. Yan, and Y. Cui, *Nat. Commun.*, **7**, 10992 (2016).
21. A. Manthiram, X. Yu, and S. Wang, *Nature Reviews Materials*, **2**, 16103 (2017).
22. A. Mauger, M. Armand, C. M. Julien, and K. Zaghib, *J. Power Sources*, **353**, 333 (2017).
23. H. Li, J. Janek, and A. Manthiram, *Solid State Ionics*, **318**, 1 (2018).
24. P. G. Bruce, S. A. Freunberger, L. J. Hardwick, and J.-M. Tarascon, *Nat. Mater.*, **11**, 19 (2012).
25. S. J. Visco, B. D. Katz, Y. S. Nimon, and L. C. De Jonghe, Li/air non-aqueous batteries. US patent 20070117007 (2007).
26. J. Zhang, W. Xu, X. Li, and W. Liu, *J. Electrochem. Soc.*, **157**, A940 (2010).
27. J. Zhang, W. Xu, and W. Liu, *J. Power Sources*, **195**, 7438 (2010).
28. J.-G. Zhang, D. Wang, W. Xu, J. Xiao, and R. E. Williford, *J. Power Sources*, **195**, 4332 (2010).

29. W. J. Kwak, H. G. Jung, D. Aurbach, and Y. K. Sun, *Adv. Energy Mater.*, **7**, 1701232, (2017).
30. W. J. Kwak, S. J. Park, H. G. Jung, and Y. K. Sun, *Adv. Energy Mater.*, **8**, 1702258 (2018).
31. D. Sharon, D. Hirschberg, M. Afri, A. Garsuch, A. A. Frimer, and D. Aurbach, *J. Phys. Chem. C*, **118**, 15207 (2014).
32. D. Sharon, M. Afri, M. Noked, A. Garsuch, A. A. Frimer, and D. Aurbach, *J. Phys. Chem. Lett.*, **4**, 3115 (2013).
33. D. Sharon, V. Etacheri, A. Garsuch, M. Afri, A. A. Frimer, and D. Aurbach, *J. Phys. Chem. Lett.*, **4**, 127 (2013).
34. D. Sharon, D. Hirschberg, M. Afri, A. Garsuch, A. A. Frimer, and D. Aurbach, *Isr. J. Chem.*, **55**, 508 (2015).
35. D. Sharon, D. Hirschberg, M. Afri, A. Garsuch, A. A. Frimer, M. Noked, and D. Aurbach, *J. Solid State Electrochem.*, **21**, 1861 (2017).
36. Y. V. Mikhaylik and J. R. Akridge, *J. Electrochem. Soc.*, **151**, A1969 (2004).
37. A. Rosenman, E. Markevich, G. Salitra, D. Aurbach, A. Garsuch, and F. F. Chesneau, *Adv. Energy Mater.*, **5**, 1500212 (2015).
38. A. Manthiram, Y. Fu, S.-H. Chung, C. Zu, and Y.-S. Su, *Chem. Rev.*, **114**, 11751 (2014).
39. E. Markevich, G. Salitra, Y. Talyosef, F. Chesneau, and D. Aurbach, *J. Electrochem. Soc.*, **164**, A6244 (2017).
40. X. Liang, C. Hart, Q. Pang, A. Garsuch, T. Weiss, and L. F. Nazar, *Nature Comm.*, **6**, 5682 (2015).
41. A. Rosenman, E. Markevich, G. Salitra, Y. Talyosef, F. Chesneau, and D. Aurbach, *J. Electrochem. Soc.*, **163**, A1829 (2016).
42. S.-H. Chung, C.-H. Chang, and A. Manthiram, *Adv. Funct. Mater.*, **28**, 1801188 (2018).
43. R. Fang, S. Zhao, P. Hou, M. Cheng, S. Wang, H.-M. Cheng, C. Liu, and F. Li, *Adv. Mater.*, **28**, 3374 (2016).
44. L. Qie, C. Zu, and A. Manthiram, *Adv. Energy Mater.*, **6**, 1502459 (2016).
45. W. Zhou, B. Guo, H. Gao, and J. B. Goodenough, *Adv. Energy Mater.*, **6**, 1502059 (2016).
46. W. Li, B. Song, and A. Manthiram, *Chem. Soc. Rev.*, **46**, 3006 (2017).
47. J. W. Choi and D. Aurbach, *Nature Rev. Mat.*, **1**, 16013 (2016).
48. C. S. Yoon, D.-W. Jun, S.-T. Myung, and Y.-K. Sun, *ACS Energy Lett.*, **2**, 1150 (2017).
49. E. Markevich, G. Salitra, F. Chesneau, M. Schmidt, and D. Aurbach, *ACS Energy Lett.*, **2**, 1321 (2017).
50. H. D. Yoo, E. Markevich, G. Salitra, D. Sharon, and D. Aurbach, *Materials Today*, **17**, 110 (2014).
51. Q. Zhong, A. Bonakdarpour, M. Zhang, Y. Gao, and J. R. Dahn, *J. Electrochem. Soc.*, **144**, 205 (1997).
52. H. Sclar, O. Haik, T. Menachem, J. Grinblat, N. Leifer, Arie Meitav, Shalom Luski, and D. Aurbach, *J. Electrochem. Soc.*, **159**, A228 (2012).
53. R. Sharabi, E. Markevich, K. Fridman, G. Gershinsky, G. Salitra, D. Aurbach, G. Semrau, M. A. Schmidt, N. Schall, and C. Bruenig, *Electrochem. Commun.*, **28**, 20 (2013).
54. Z. H. Lu, L. Y. Beaulieu, R. A. Donaberger, C. L. Thomas, and J. R. Dahn, *J. Electrochem. Soc.*, **149**, A778 (2002).
55. Y.-K. Sun, *Nat. Mater.*, **8**, 320 (2009).
56. Y. K. Sun, S. T. Myung, M. H. Kim, J. Prakash, and K. Amine, *J. Am. Chem. Soc.*, **127**, 13411 (2005).
57. D. W. Jun, C. S. Yoon, U. H. Kim, and Y. K. Sun, *Chem. Mater.*, **29**, 5048 (2017).
58. S. T. Myung, F. Maglia, K. J. Park, C. S. Yoon, P. Lamp, S. J. Kim, and Y. K. Sun, *ACS Energy Lett.*, **2**, 196 (2017).
59. C. S. Yoon, H. H. Ryu, G. T. Park, J. H. Kim, K. H. Kim, and Y. K. Sun, *J. Mater. Chem. A*, **6**, 4126 (2018).
60. W. Liu, P. Oh, X. Liu, M.-J. Lee, W. Cho, S. Chae, Y. Kim, and J. Cho, *Angew. Chem., Int. Ed.*, **54**, 4440 (2015).
61. F. Schipper, E. M. Erickson, C. Erk, J.-Y. Shin, F. F. Chesneau, and D. Aurbach, *J. Electrochem. Soc.*, **164**, A6220 (2017).
62. J. Xu, F. Lin, M. M. Doeff, and W. Tong, *J. Mater. Chem. A*, **5**, 874 (2017).
63. H. Kim, M. G. Kim, H. Y. Jeong, H. Nam, and J. Cho, *Nano Lett.*, **15**, 2111 (2015).
64. H. J. Noh, S. Youn, C. S. Yoon, and Y. K. Sun, *J. Power Sources*, **233**, 121 (2013).
65. D. J. Miller, C. Proff, J. G. Wen, D. P. Abraham, and J. Bareno, *Adv. Energy Mater.*, **3**, 1098 (2013).
66. F. A. Susai, H. Sclar, Y. Shilina, T. R. Penki, R. Raman, S. Maddukuri, S. Maiti, Ion C. Halalay, S. Luski, B. Markovsky, and D. Aurbach, *Adv. Mater.*, 1801348 (2018).
67. G. Salitra, E. Markevich, M. Afri, Y. Talyosef, P. Hartmann, J. Kulisch, Y.-K. Sun, and D. Aurbach, *ACS Appl. Mater. Interfaces*, **10**, 19773 (2018).
68. M. S. Park, S. B. Ma, D. J. Lee, D. Im, S.-G. Doo, and O. Yamamoto, *Sci. Rep.*, **4**, 3815 (2015).
69. E. Kazyak, K. N. Wood, and N. P. Dasgupta, *Chem. Mater.*, **27**, 6457 (2015).
70. G. Bieker, M. Winter, and P. Bieker, *Phys. Chem. Chem. Phys.*, **17**, 8670 (2015).
71. E. Markevich, K. Fridman, R. Sharabi, R. Elazari, G. Salitra, H. E. Gottlieb, G. Gershinsky, A. Garsuch, G. Semrau, M. A. Schmidt, and D. Aurbach, *J. Electrochem. Soc.*, **160**, A1824 (2013).
72. H. Nakai, T. Kubota, A. Kita, and A. Kawashima, *J. Electrochem. Soc.*, **158**, A798 (2011).
73. K. Leung, S. B. Rempe, M. E. Foster, Y. Ma, J. M. Martinez del la Hoz, N. Sai, and P. B. Balbuena, *J. Electrochem. Soc.*, **161**, A213 (2014).
74. I. Shkrob, J. F. Wishart, and D. P. Abraham, *J. Phys. Chem. C*, **119**, 14954 (2015).
75. E. Markevich, G. Salitra, K. Fridman, R. Sharabi, G. Gershinsky, A. Garsuch, G. Semrau, M. A. Schmidt, and D. Aurbach, *Langmuir*, **30**, 7414 (2014).
76. E. Markevich, G. Salitra, and D. Aurbach, *ACS Energy Lett.*, **2**, 1337 (2017).
77. K. Fridman, R. Sharabi, R. Elazari, G. Gershinsky, E. Markevich, G. Salitra, D. Aurbach, A. Garsuch, and J. Lampert, *Electrochem. Commun.*, **33**, 31 (2013).
78. K. Fridman, R. Sharabi, E. Markevich, R. Elazari, G. Salitra, G. Gershinsky, D. Aurbach, J. Lampert, and M. Schulz-Dobrick, *ECS Electrochem. Lett.*, **2**, A84 (2013).
79. E. Markevich, R. Sharabi, H. Gottlieb, V. Borgel, K. Fridman, G. Salitra, D. Aurbach, G. Semrau, M. A. Schmidt, and N. Schall, N, and C. Bruenig, *Electrochem. Commun.*, **15**, 22 (2012).
80. E. Markevich, G. Salitra, Y. Talyosef, U.-H. Kim, H.-H. Ryu, Y.-K. Sun, and D. Aurbach, *ACS Applied Energy Materials*, **1**, 2600 (2018).
81. J. Xu, E. Hu, D. Nordlund, A. Mehta, S. N. Ehrlich, X.-Q. Yang, and W. Tong, *ACS Appl. Mater. Interfaces*, **8**, 31677 (2016).
82. J. Xu, F. Lin, D. Nordlund, E. J. Crumlin, F. Wang, J. Bai, M. M. Doeff, and W. Tong, *Chem. Commun.*, **52**, 4239 (2016).
83. S. Yoon, K. J. Park, U.-H. Kim, K. H. Kang, H.-H. Ryu, and Y.-K. Sun, *Chem. Mater.*, **29**, 10436 (2017).
84. U.-H. Kim, E.-J. Lee, C. S. Yoon, S.-T. Myung, and Y.-K. Sun, *Adv. Energy Mater.*, **6**, 1601417 (2016).
85. H.-H. Ryu, K. J. Park, C. S. Yoon, and Y.-K. Sun, *Chem. Mater.*, **30**, 1155 (2018).
86. K. J. Park, M. J. Choi, F. Maglia, S. J. Kim, K. H. Kim, C. S. Yoon, and Y. K. Sun, *Adv. Energy Mater.*, **8**, 1703612 (2018).
87. D. Aurbach, *J. Power Sources*, **89**, 206 (2000).
88. J. Li, L. E. Downie, L. Ma, W. Qiu, and J. R. Dahn, *J. Electrochem. Soc.*, **162**, A1401 (2015).
89. E. Cho, S.-W. Seo, and K. Min, *ACS Appl. Mater. Interfaces*, **9**, 33257 (2017).
90. C. S. Yoon, M. H. Choi, B.-B. Lim, E.-J. Lee, and Y.-K. Sun, *J. Electrochem. Soc.*, **162**, A2483 (2015).
91. S. Watanabe, M. Kinoshita, T. Hosokawa, K. Morigaki, and K. Nakura, *J. Power Sources*, **258**, 210 (2014).
92. T. Hayashi, J. Okada, E. Toda, R. Kuzuo, N. Oshimura, N. Kuwata, and J. Kawamura, *J. Electrochem. Soc.*, **161**, A1007 (2014).
93. K. J. Park, H. G. Jung, L. Y. Kuo, P. Kaghazchi, C. S. Yoon, and Y. K. Sun, *Adv. Energy Mater.*, **8**, 1801202 (2018).
94. S. J. Park, J. Y. Hwang, C. S. Yoon, H. G. Jung, and Y. K. Sun, *ACS Appl. Mater. Interfaces*, **10**, 17985 (2018).
95. M. Dixit, B. Markovsky, D. Aurbach, and D. T. Major, *J. Electrochem. Society*, **164**, A6359 (2017).
96. F. Schipper, H. Bouzaglio, M. Dixit, E. M. Erickson, T. Weigel, M. Talianker, J. Grinblat, L. Burstein, M. Schmidt, J. Lampert, C. Erk, B. Markovsky, D. T. Major, and D. Aurbach, *Adv. Energy Mater.*, **8**, 1701682 (2018).
97. U.-H. Kim, D.-W. Jun, K.-J. Park, Q. Zhang, P. Kaghazchi, D. Aurbach, D. T. Major, G. Goobes, M. Dixit, N. Leifer, C. M. Wang, P. Yan, D. Ahn, K.-H. Kim, C. S. Yoon, and Y.-K. Sun, *Energy Environ. Sci.*, **11**, 1271 (2018).
98. E. A. Olivetti, G. Ceder, G. G. Gaustad, and X. Fu, *Joule*, **1**, 229 (2017).
99. S. Jaffe, *Joule*, **1**, 220 (2017).
100. D. B. Wellbeloved, P. M. Craven, and J. W. Wauily, in *Ullmann's Encyclopedia of Industrial Chemistry*, 5th edition, B. Elvers, S. Hawkins, and G. Schulz, Editors, V. A16, p.79, Wiley-VCH, Weinheim (1990).
101. D. G. E. Kerfoot, in *Ullmann's Encyclopedia of Industrial Chemistry*, 5th edition, B. Elvers, S. Hawkins, and G. Schulz, Editors, V. A17, p. 160, Wiley-VCH, Weinheim (1991).
102. A. Banerjee, B. Ziv, Y. Shilina, S. Luski, D. Aurbach, and I. C. Halalay, *ACS Energy Lett.*, **2**, 2388 (2017).
103. A. Banerjee, B. Ziv, S. Luski, D. Aurbach, and I. C. Halalay, *J. Power Sources*, **341**, 457 (2017).